COMPUTER APPLICATIONS IN DIRECTIONAL SOLIDIFICATION PROCESSING

A. F. Giamei and J. S. Erickson

Materials Engineering and Research Laboratory
Pratt & Whitney Aircraft, East Hartford, CT 06108

ABSTRACT

Directional solidification has progressed from the laboratory stage to the production floor within the last decade. Applications include directionally solidified superalloys in the form of columnar grained gas turbine airfoils, and could eventually extend to eutectics and single crystal superalloys. Computers have played a significant role in the rapid evolution of directional solidification processing methods. Computer applications in this field can be broken down into three major areas. The first is computerized thermal analysis of cooling curves in order to quickly and accurately obtain solidification parameters such as growth rate, thermal gradient, cooling rate, etc. The second is computer modeling of the heat flow problem associated with unidirectional solidification. Various models have been used in this connection, including finite difference, finite element and one dimensional steady state approximations. Each has its own advantages and shortcomings and these will be discussed in some detail. The third and final area is computer control. The use of direct digital or analog control can lead to highly reproducible thermal conditions which can be used to grow superalloys or modern eutectic composites.

Introduction

Advanced gas turbine requirements have necessitated the development of a new manufacturing process, namely directional solidification. The hottest and most highly stressed components in the gas turbine perform better when cast as air cooled airfoils without grain boundaries perpendicular to the principal stress axis. The advantages of columnar grain structure in Ni-base superalloys under uniaxial load at high temperature were pointed out by VerSnyder in 1959 (1). The further advantages of superalloy single crystals were discussed in 1967 (2) and the fabrication method for both [100] columnar grained and [001] single crystal turbine blades was summarized by VerSnyder and Shank in 1970 (3). This original directional solidification method was known as power-down since the solidification cycle was controlled by gradually reducing the power to the upper portion of a resistance or an induction heater. This process was limited to low and varying thermal gradients due to the variable length of the heat conduction path between the solidus isotherm and the water cooled copper chill plate at the bottom of the castings. Defects such as equiaxed grain or "freckles" were observed (4, 5) and were primarily attributable to low thermal gradients. Thermally, the power-down process is nearly identical with the original exothermic process introduced by Flemings in 1961 (6).

A significantly higher thermal gradient process, namely HRS or High Rate Solidification was introduced in 1971 (7). The removal of heat in this process was primarily controlled by radiation from the shell mold to the vacuum chamber walls. This led to less spatial variation in solidification parameters as well as a process with improved economics. This process is primarily one in use for the production of cube textured directionally solidified gas turbine airfoils. Freckles, hot-tearing and equiaxed grains occur only rarely in most cored airfoils with proper baffling and process control.

The arrival of eutectics on the scene by 1971 (8) as serious gas turbine airfoil candidates required dramatic improvements in thermal conditions for directional solidification processing. Bridgman bar growth using a water spray for extremely effective cooling was used with a protective atmosphere (9). Complex airfoil shapes could be grown under vacuum as well as argon with the LMC (Liquid Metal Cooling) process (10). These conductive and convective cooling methods led to substantial improvement in thermal gradient as shown in Figure 1. The high thermal gradient requirement is justified in Figure 2. Many advanced eutectic alloys have a critical ratio of thermal gradient (G) to growth Rate (R) in excess of 1500°F hr/in^2 (130°C hr/cm^2) requiring a thermal gradient of at least 1500°F/in (328°C/cm)to grow at a rate of 1 in/hr (2.54 cm/hr) with a fully plane front microstructure. Coupled growth of the matrix and the reinforcing phase leads to microstructures such as that shown in Figure 3.

I. Computerized Thermal Analysis

The first step in improving a process is knowing where you are to begin with. The following method of directional solidification thermal analysis has yielded the fruits of success in documentation of solidification parameters. The first step is to obtain cooling curves, temperature (T) vs. time (t). This can be done by arranging a linear array of thermocouples on the outside of the mold or within the melt along the desired direction of growth, as in Figure 4. The position of each thermocouple bead relative to a reference position (the chill plate or the bottom of the mold) must be recorded. We have found the platinum-6% Re vs. platinum-30% Re to be most satisfactory in high temperature high vacuum work.

The thermocouple EMF may then be recorded on a multi-channel recorder as a function of time after the start of the controlled solidification cycle.

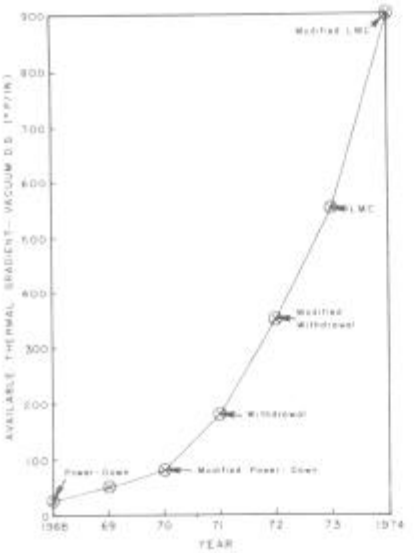

Figure 1. Historical trend for thermal gradient associated with directional solidification.

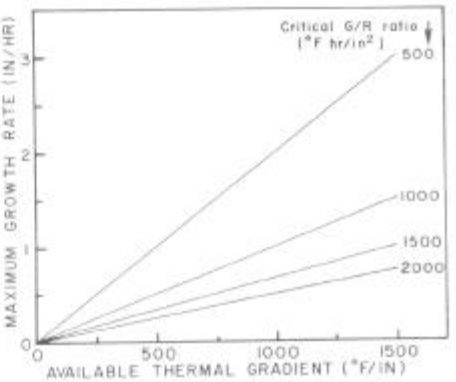

Figure 2. Relationship between maximum permissible growth rate and available thermal gradient with critical G/R (Gradient to Rate) ratio as parameter.

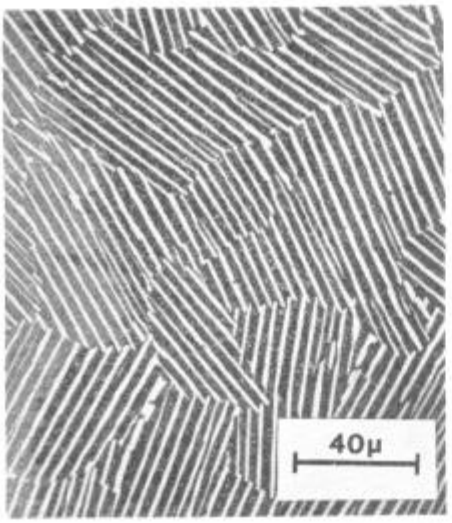

Figure 3a. Transverse metallographic section of Ni-19.7Cb-2.5Al-6Cr (wt%) grown at 0.75 in/hr showing grain structure and phase morphology.

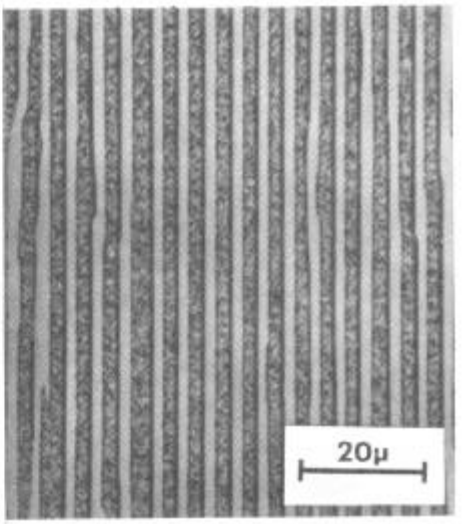

Figure 3b. Longitudinal section of lamellar eutectic showing distribution of reinforcing phases. Grown in the vertical sense at 0.75 in/hr.

If a temperature-time recorder is used, this information can be coded and keypunched for execution by the PROCES program written for the IBM-370 system. If only EMF is available, that information can also be coded and keypunched for input into a pre-processor known as PROCESIN which converts the EMF vs. time and position table into temperature in °F or °C, as desired. This information can be reviewed or fed directly into PROCES.

The main program examines the cooling curves at one point in time and draws a temperature-distance profile for each time which is curve fitted with a second order polynomial in distance (Z) for 3 or 4 channels of input, or a third order polynomial in Z for 5 to 8 channels of temperature input. A schematic of these temperature profiles is shown in Figure 5. If the isotherm of interest is now superimposed (Liquidus Temperature, T_L, Solidus Temperature, T_S or Eutectic Temperature, T_E), the interface position can be obtained by iterative interpolation. The slope of the continuous temperature profile at that point can now be obtained by differentiation and this gives the thermal gradient at the selected isotherm and time.

The next step is illustrated in Figure 6 where the interface positions obtained previously are now plotted as a function of time. This plot contains a great deal of useful information. When the liquidus and solidus growth curves are plotted up for the case of dendritic growth and curve fitted with a third order polynomial in time, the growth rate of the respective isotherm can be obtained by differentiation and evaluated at any time. The vertical separation (ΔZ) between these curves is inversely related to the thermal gradient as follows:

$$G = \frac{\Delta T}{\Delta Z} = \frac{T_L - T_S}{Z_L - Z_S} \qquad (1)$$

and the horizontal separations is the local solidification time, Δt which relates to the cooling rate, $\dot{T}$, as follows (11):

$$\Delta t = \frac{\Delta T}{\dot{T}} = \frac{\Delta T}{RG} \qquad (2)$$

This time, in turn correlates with the secondary dendrite arm spacing (S_2) as follows (12):

$$S_2 \propto (\Delta t)^n, \; 1/3 \leq n \leq 1/2 \qquad (3)$$

All the fundamental solidification quantities can be obtained from this one plot!

For convenience, thermal gradient is next plotted as a function of distance. The next plot is growth rate vs. distance. Since growth rate and thermal gradient have intentionally been measured at the same interface positions, they can now be cross plotted as a linear Rate-Gradient map. An example is shown in Figure 7 of actual Calcomp computer output. Several structural requirements can immediately be checked from this diagram. For example, our experience indicates that $G/R \leq 3$ °F-hr/in^2 (0.26 °C-hr/cm^2) always leads to the columnar-equiax transition, and $G/R \geq 5$ (0.43°C-hr/cm^2) rarely has given equiaxed grain in most Ni-base superalloys. Furthermore, $G \geq 80$°F/in (17.4°C/cm) will normally guarantee no "freckles" in alloys such as Mar-M200. A further no-freckling requirement is that $\dot{T} = RG \geq 1000$°F/hr (550°C/hr), in the case of Mar-M200. One can also determine the fineness of the dendritic structure (see Eq. 2 and 3) and the refinement of coupled growth structures (see Figure 3).

The final two plots are of mushy zone height vs. distance solidified and local solidification time vs. distance. These plots are convenient in order

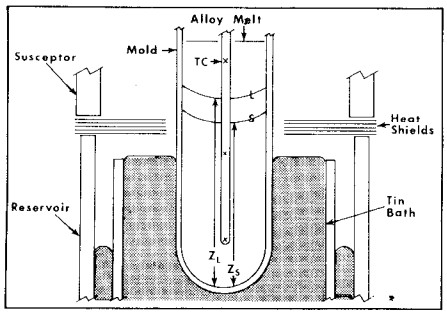

Figure 4. Schematic diagram of LMC laboratory unit. Only the region of sharp temperature transition is shown. Liquidus and Solidus positions (Z) are shown for a typical Ni-base superalloy and an intermediate immersion rate.

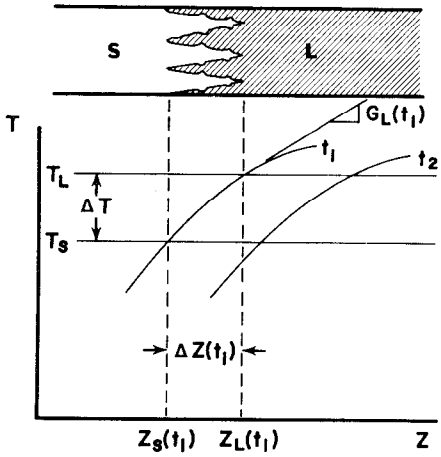

Figure 5. Schematic drawing of Temperature (T) vs. distance (Z) for two different times (t). The melting range, mushy zone height and thermal gradient in the liquid at time t_1 are indicated.

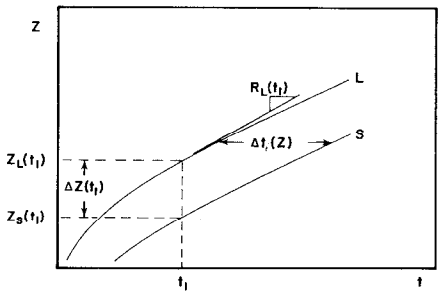

Figure 6. Schematic drawing of interface position (Z) vs. time (t) for the liquidus and solidus isotherms. The mushy zone height, local solidification time and growth rate of the liquidus surface at time t_1 are indicated.

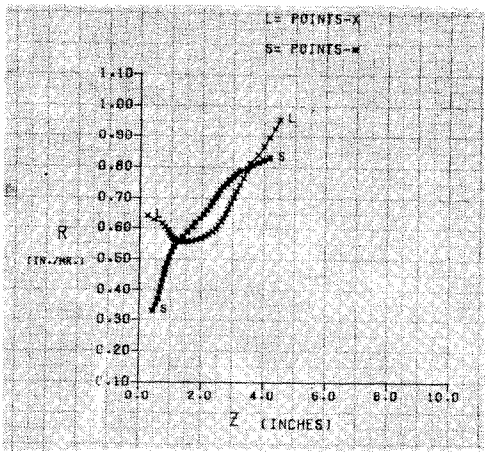

Figure 7. Calcomp plot of growth rate (R) vs. thermal gradient (G) for both liquidus and solidus surfaces. The thermal analysis has been carried out for an LMC run at relatively low superheat.

to compare alloys or process changes. The mushy zone height (ΔZ) is inversely related to the thermal gradient as shown in Eq. 1. Many superalloys have 200-300°F (110-165°C) melting ranges which in practice lead to substantial mushy zone height, e.g. 1-2 in (2.5 - 5 cm). Anything above 2 inches (5 cm) would be considered excessive and prove very difficult to feed in order to avoid hot tearing in crack-prone geometries. In terms of local solidification time, anything in excess of 15 minutes would be considered unnecessarily long and can lead to mold-metal reaction or freckling.

The cost of this entire analysis has dropped over the past seven years by around 70% due to the advent of very high speed time sharing digital computers. The execution time would normally be under 15 seconds of IBM-370 time and the program is only recompiled when there are updates.

Perhaps the most exciting recent development in the area of thermal data reduction has been the use of an interactive mode of analysis. This reduces the so called "turnaround time" from up to two days for a batch job (cards) to a few minutes, depending on requirements. Another advantage is the opportunity for on-line data correction. The combination of virtual storage and a Cathode Ray Tube display system allows the user to re-plot crowded figures using a portion of the data on each sub-plot. The cost for this method of analysis is truly inconsequential.

II. Computer Modeling of Directional Solidification

1.) Finite Element Method

Both the power down process and the High Rate Solidification process previously described have been analytically treated utilizing a two-dimensional, transient, finite element, heat transfer computer program. This program can take into account both time-varying boundary conditions and temperature-dependent thermal properties for both alloy and mold materials. Since the particular analysis utilized was limited to a two-dimensional solution, the casting process was evaluated on unidirectionally solidified ingots of Mar-M200, which provided the required axis of symmetry. In the analysis, the temperature profiles on the external mold surface, upper alloy melt surface, and chill plate surfaces were experimentally measured during the entire solidification process and were inputted into the computer program as boundary conditions (13).

The finite element nodal break-up employed is shown in Figure 8. The break-up problem can be done by a stress deck. A total of 798 nodal elements were utilized to provide the necessary spatial break-up. A typical finite element run requires 1-3 min of IBM-370 time.

Figure 9 shows plots of the liquidus and solidus isotherms along the centerline of a three inch (7.62 cm) diameter directionally solidified Mar-M200 ingot made by the power down process. Superimposed on the same graph are the locations of the same isotherms on the outer mold surface. The two major points that can be obtained from this analysis is that the rate of progression of the solidification front is quite rapid adjacent to the chill surface but quickly diminishes as the conductive path becomes larger. In addition early in the solidification cycle it is obvious that a thermal lag exists between the outer mold surface and the ingot centerline, at least for a 3 inch diameter cylinder. The finite element heat transfer analysis, being two dimensional, clearly shows how this thermal lag affects solid-liquid interface curvature as shown in Figure 10. At 15 minutes after pour the solid-liquid interface exhibits a concave downward interface indicating the strong influence that conduction to the chill has on interface curvature. When the interface has moved further upward the conductive path between the chill and interface increases resulting in a broadening of the mushy zone. Eventually a point is reached (150 minutes) in the process where the ingot surface cools rapidly as a result of a reduction in power

to the upper coil. This results in a change in interface curvature from concave to convex downward. This change in curvature corresponds to the cross-over in mold wall and alloy centerline isotherms shown in Figure 9. If this cooling effect is sufficiently large, sidewall nucleation can occur resulting in the formation of equiaxed grains and the loss in directionality. This points out one of the major deficiencies in the power down process, namely, the inability to sustain directional growth over large distances.

The High Rate Solidification process, on the other hand, relies on a mold translation technique to achieve additional radiative cooling. In this case as the mold exits the hot zone cooling of the solid portion of the casting occurs by conduction to the chill as well as radiation from the mold surface. Figure 11 shows the heat transfer conditions which prevail along the centerline of a 3 inch (7.62 cm) Mar-M200 ingot directionally solidified with the HRS process. As in the case of the power down casting previously described the boundary conditions were experimentally determined by thermocouples attached to the chill surface, outer mold surface, and upper melt surface and inputted into the two dimensional finite element program. Examination of Figure 11 shows that in the case of the HRS process there exist two predominant heat transfer regimes. Adjacent to the chill surface there is a chill dominant region wherein heat transfer occurs by conduction to the chill. As the distance between the solidifying front and the chill increases the role that conduction plays in the process is diminished. Beyond a certain point in the casting cycle, typically 2-3 inches of growth, a withdrawal dominant heat transfer regime exists wherein radiative heat transfer is the predominant heat transfer mechanism. In this regime a steady state heat transfer situation is approached where the rate of motion of the solidification front approximates the translation rate. This permits directional growth to be sustained over substantial distances, e.g. 16-24 inches. Higher temperature gradients and smaller mushy zone widths are additional benefits associated with the HRS process.

Another interesting application of finite element heat transfer is the determination of solid-liquid interfacial curvature as it progresses through the cross sectional area changes characteristic of turbine airfoils. Figure 12 illustrates a cross sectional area change representative of the type found in going from the airfoil section of a blade into a larger area such as a blade shroud or root section. It can be seen that in one instance a convex downward interface exists through the transition region which can cause separate grain nucleation. The random nucleation of grains is considered undesirable since it can result in grains which do not possess the desired [100] crystallographic orientation(14). By suitable adjustment of solidification conditions a horizontal or concave downward interface can be obtained which will aid in preventing separate grain nucleation. One therefore can use the finite element technique to gain a better appreciation of the solid-liquid interface curvature effects which exist during unidirectional solidification of complex shapes.

2) Finite Difference and Analog Methods

Both the power-down and LMC directional solidification processes have been analyzed by the finite difference method. This approach reduces the heat transfer problem to a system of finite difference equations and iteratively approaches a steady state (15). In our work, we used a "TOSS" (Transient or Steady State) deck which required prior break-up of the body, e.g. as shown in Figure 13 for the case of a round bottom recrystallized alumina mold with a thermocouple protection tube along the centerline. The set-up is for the LMC process. The material properties can be assigned as a function of temperature, e.g. as in the case of the alloy specific heat in order to take the heat of fusion into account.

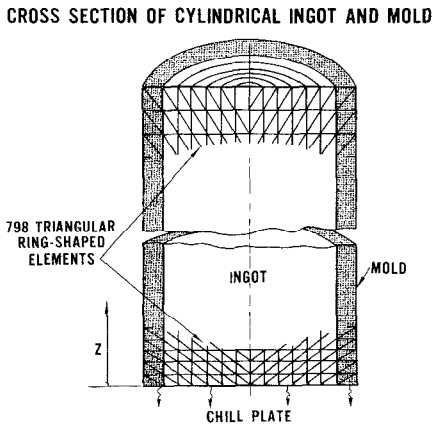

Figure 8. Diagram showing breakup method for finite element analysis of circular cylinder.

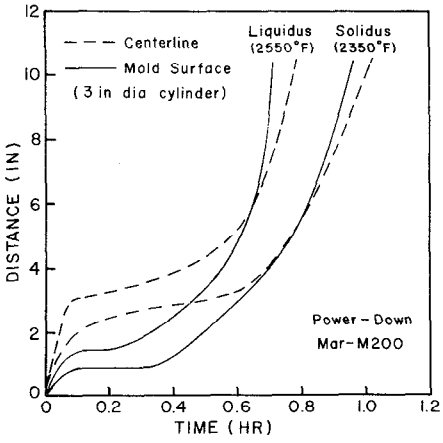

Figure 9. Computed distance-time curves for a cylindrical ingot using the finite element method.

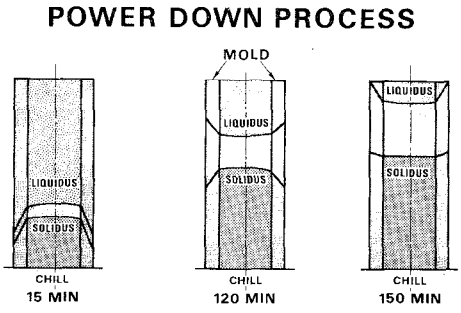

Figure 10. Finite element results for circular ingot grown by the power-down method. Note the changes in interfacial curvature in the alloy as a function of time.

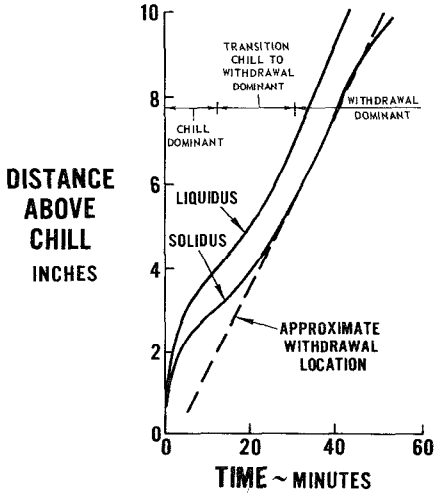

Figure 11. Computed distance-time curves for the withdrawal process using the finite element method.

For non-steady shapes, we found the finite difference method to be slow in terms of execution time (15-20 min), but very useful due to the time dependence and multi- dimensional nature of the output. For example, in Figure 14 the shape of the liquidus and solidus isotherms can be envisaged, as well as the depth of the "mushy" zone (liquid + solid). These steady state shapes were computed at various immersion rates for the mold. The significant findings were that the LMC process had the potential for extremely high thermal gradient and very flat interfaces over a wide range of immersion (growth) rates. The interfaces were convex up at 0-20 in/hr (0-51 cm/hr), very flat from 20-40 in/hr and concave up above 40 in/hr (101.6 cm/hr). The thermal gradient ranged from 457 - 1371°F/in (100-300°C/cm), depending on assumed conditions. It soon became obvious that the susceptor was not at a uniform temperature, because the measured thermal gradients were lower than calculated using a uniform hot zone. This was later verified experimentally.

Computations for LMC also demonstrated that the lead of the solidus isotherm relative to the coolant level decreased as the immersion rate increased. Typical lead distances of 0.2-1.0 in (0.5-2.5 cm) were subsequently verified. Further calculations predicted the low sensitivity of thermal gradient to immersion rate, mold thickness and mold conductivity. Despite the slow rate of convergence of the program, many experiments were done on the computer with a substantial time and cost savings. This was a particularly useful method because of the detailed information which it provided and since so little was known about the characteristics of the LMC process at the time the finite difference program was being used.

Finite difference had previously been applied to the power-down process with little advantage relative to the finite element results. However, the comparison of these two methods with the analog method can be made in this case. Here the body is reduced to a network of capacitances and resistances and the electrical analog simulation is readily solved (16) by conventional means. In our case, a fine nodal network was used and the analog method required 12 minutes of execution time, a slight advantage relative to finite difference. However, there are obvious errors in the analog solutions for transient conditions (e.g. near the chill plate) or for variations in the density of nodes. For our purposes, the analog method was least desirable and was only used as a check on the finite element and finite difference results.

3) Analytical Method

Perhaps the most useful technique in our endeavors has been the analytical or closed form or one dimensional steady state approximation method (17). Here, based on the knowledge gleaned from the previously outlined computer methods and experimental information, we assume that heat flows uniaxially across the isotherm(s) of special interest, e.g. solidus and liquidus or eutectic temperatures. A one dimensional heat flow calculation presumes a constant cross-section. However, if we use the extended heat equation with sources and sinks along the Z axis, we can take into account radial heat flow away from the solidification interface. For example, in the hot zone, the radiative flux can be computed as received from the susceptor with the appropriate view factor, conducted through the cylindrical mold wall, and collapsed to a point or line source of equivalent heat flux along the mold axis. Radial heat flow to the coolant can be accomodated in a similar manner, where a heat sink is now used. The heat of fusion is again taken into account in the specific heat. A closed form solution can now be obtained (17).

There were two immediate applications for these computations. The first problem was to assess the utility of LMC at high growth rate. In this case we were interested in growing Ni-base superalloy crystals at well above the usual growth rates of 4-12 in/hr (10-30 cm/hr). The early cal-

culations indicated that there was no substantial decrease in available thermal gradient out to 100 in/hr (254 cm/hr). This was verified by experimental measurement and by the fact that superalloy crystals have been grown with LMC out to rates of 200 in/hr (508 cm/hr).

The second application was to the problem of eutectic solidification. Here the name of the game was to achieve high thermal gradient in order to obtain plane front growth at the highest possible rates. Thousands of computer experiments could now be done in three or four minutes of execution time and they were! The payoff was almost immediate. By careful examination of the results of single, double and even triple parametric variations, promising combinations were identified and tried. The thermal gradient was soon raised from 585°F/in (130°C/cm) to 900°F/in (200°C/cm).

Consider some of the results of single parametric variations. A base case was assumed with a hot zone temperature of 2700°F (1482°C). This is not necessarily the peak temperature, but rather the average temperature just above the baffle region. The eutectic temperature was taken as 2300°F (1260°C). The baseline coolant temperature was assumed to be 600°F (315°C), an average just below the baffles. The baffle height was taken as 0.3 in (0.76 cm) and the rate as 1 in/hr (2.5 cm/hr). The surface to volume or perimeter to area ratio was taken as 8 in^{-1} (3.2 cm^{-1}), typical of a 0.5 in (1.27 cm) dia. bar or of many turbine airfoils, and some root sections. The mold was taken as 0.1 in (0.25 cm) of fully dense aluminum oxide and the heat transfer coefficient was chosen to be conservatively low for a slowly circulating tin bath. (The circulation was mainly used to prevent thermal layering by constantly displacing the hottest tin out of the vicinity of the mold).

Consider the result in Figure 15. The conclusion is that thermal gradient is relatively insensitive to immersion rate over the range of interest for eutectics. This was a significant and encouraging result. (The baseline condition is indicated by an arrow in this and subsequent figures in this section). Note that the calculated thermal gradient of 1040°F/in (230°C/cm) is essentially equivalent to measured values of 800-1000°F/in (178-222°C/cm). This is arranged by the proper selection of hot zone and coolant temperatures. However, this is not a totally forced situation. Namely, if a choice of higher coolant temperatures than experimentally measured is required for agreement, this may mean that poor coolant circulation is occurring in the real system. In this manner we became aware of experimental problems. The slight positive slope in Figure 15 is due to the fact that the interface moves toward the baffles at the higher rates and this is the region where temperature varies most rapidly with distance in the casting, therefore a slight thermal gradient enhancement is noted.

Figure 16 shows the computed relationship between the position of the interface (above the tin level) as a function of the height or thickness of the baffle. The result is a monotonic increase in interface position with increasing baffle height, as one might expect. However, the lead distance from the eutectic interface to the top of the baffle is less for thicker baffles.

Probably the most significant finding is shown in Figure 17, a plot of thermal gradient in the liquid at the eutectic temperature as a function of effective hot zone temperature. The thermal gradient monotonically increases with hot zone temperature, in agreement with experience. The key point, however, is that we are dealing with a heat input limited process. This is consistent with the high potency of available cooling and the fact that the interface is above the baffle.

Figure 18 is very important from a practical point of view. In this case the available thermal gradient is shown to increase as the P/A (Perimeter to

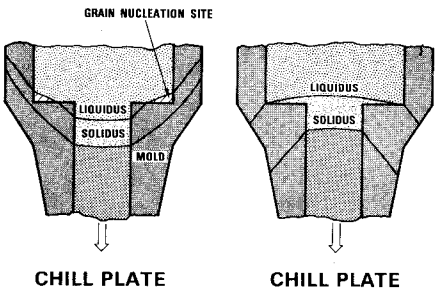

Figure 12. Results from finite element calculations for change in cross-sectional area. Note that when the interface curves upwards there is a potential grain nucleation problem.

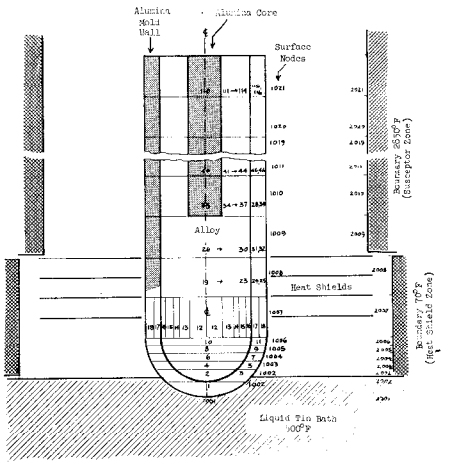

Figure 13. Drawing showing break-up details for finite difference calculations on round bottom cylinder. Boundary conditions are also given in the hot zone and in the baffle region.

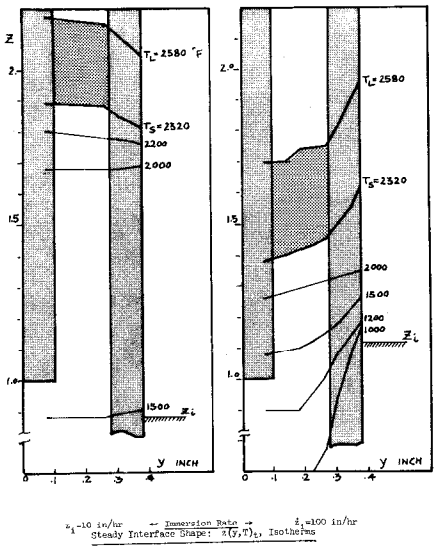

$\dot{z}_i$=10 in/hr ← Immersion Rate → $\dot{z}_i$=100 in/hr
Steady Interface Shape: $z(y,t)_i$, Isotherms

Figure 14. Results from finite difference computations showing interface curvature effects at two different immersion rates.

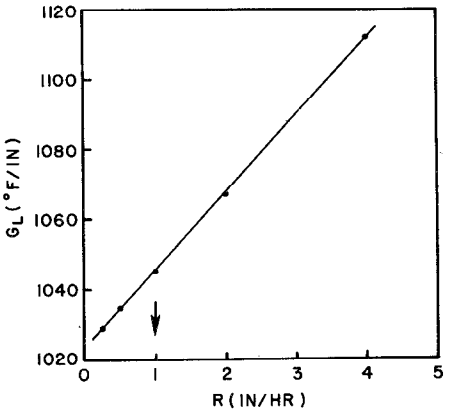

Figure 15. Thermal gradient at the eutectic isotherm as a function of immersion rate for the LMC process. These computed results are from a one dimensional steady state model. Note the expanded scale on the vertical axis.

Area) ratio of the transverse section of the solidified body increases. The reasoning is that more surface area allows more efficient heating in the hot zone and the eutectic interface is pushed down toward the baffle zone where temperature varies most rapidly with distance, and therefore a higher thermal gradient is achieved. The implication is that large section sizes will normally be associated with low thermal gradient and that for a given cross sectional area, a circular cylinder represents the most difficult shape for obtaining high thermal gradient values. In a multi-section body such as a gas turbine blade, the airfoil should be somewhat easier than the thicker root section to grow with a planar front microstructure.

The position of the eutectic interface is plotted against the heat transfer coefficient in Figure 19. Again the results are consistent with the conclusion that we are dealing with a heat input limited process. Even moderate cooling pushes the interface well up into the hot zone and the effect quickly saturates out. Good cooling efficiency is only required at the higher immersion rates (e.g. for superalloys) or for higher hot zone temperatures (very high thermal gradient). It can also be seen that the coolant bath temperature plays only a minor role in terms of thermal gradient or interface position, again because the conditions selected for analysis are not very stringent with respect to the coolant. There is therefore no requirement to vigorously agitate the coolant, but rather just to stir it in order to preserve uniformity of temperature.

There are other variables of interest concerning the mold itself, namely the thickness and thermal conductivity. Figure 20 indicates that the thermal gradient in the liquid decreases with increasing mold thickness. A thin mold is helpful in getting the heat into the metal above the baffle and in removing heat in the region below the baffle. A very similar effect is observed in terms of the thermal conductivity of the mold. The more conductive the mold material, the easier it is to add heat above the baffle and remove it below. The important quantity to be minimized is the mold thermal resistance in order to achieve high thermal gradient. See also Figure 21.

III. Experimental vs. Analytical Comparison

In section II-3 a one dimensional dynamic steady state heat transfer model was discussed in detail. This model has been effectively utilized in the analysis of the liquid metal cooling process as it applies to eutectic turbine blade solidification. Figure 22 is a schematic of the liquid metal cooling furnace utilizing a refractory metal chill plate. This furnace has been employed to cast $\gamma/\gamma' + \delta$ eutectic turbine blades. The LMC process (18) has been selected for this application because of its ability to produce the high temperature gradients required to sustain plane front growth. Tin is utilized as the quenching media due to its low melting point 450°F (232°C), its vapor pressure characteristics which are compatible with vacuum operation, its good thermal properties, excellent convective characteristics, and reasonable cost. A more complete processing description of the unidirectional solidification of eutectic turbine blades is beyond the scope of this paper but has been treated in greater detail elsewhere (18).

From a computer modeling standpoint the one dimensional dynamic steady state analysis can be applied to the growth of complex geometries. Therefore it is useful as a predictive tool in understanding the relationship between casting process parameters and heat transfer conditions such as temperature gradient and solidification rate.

For example, from a heat transfer standpoint the geometry of a particular cross section in a blade casting can be characterized by the ratio of casting perimeter to cross sectional area (P/A ratio). This would be the same as the surface to volume ratio for a constant cross section. Since the one dimensional model is a steady state analysis, it is limited to consideration of a constant P/A ratio shape. However, as a first approximation the results

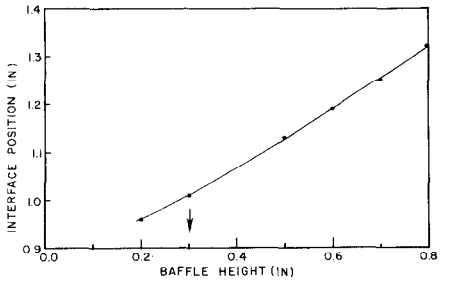

Figure 16. Analytical results from one dimensional dynamic steady state heat transfer model. The location of the 2300 °F eutectic isotherm is plotted as a function of the height of the lower baffle system. The base case condition is indicated by an arrow. The origin of the vertical axis is at the top of the coolant bath.

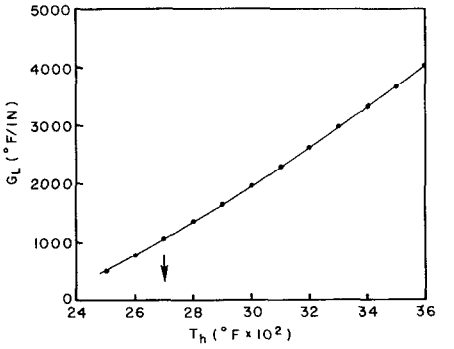

Figure 17. Analytical results for thermal gradient in the liquid at the eutectic temperature as a function of hot zone temperature. The thermal gradient increases markedly as hot zone temperature increases.

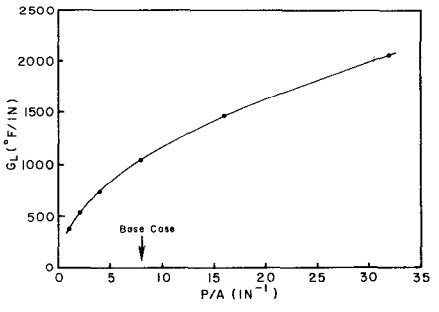

Figure 18. Analytical results for thermal gradient as a function of perimeter to area ratio for a body of constant cross section. The base case represents a circular cylinder with 0.5 inch diameter.

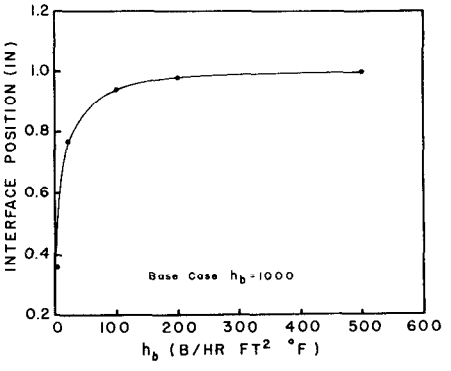

Figure 19. Analytical results for eutectic isotherm location as a function of heat transfer coefficient to the cooling bath.

calculated for P/A ratios typical of blade root and airfoil sections may be combined to predict the thermal events which occur at the cross sectional area change as described below.

Figure 23 is a plot showing the location of the solid-liquid interface relative to the radiation baffle for P/A ratios typical of blade airfoil (P/A = 15 in^{-1}) and blade root (P/A = 5 in^{-1}) sections. It can be seen that over a large range of furnace hot zone temperatures the steady state location of the solid-liquid interface in the airfoil section is closer to the radiation baffle than that of the root. Therefore, as the solid-liquid interface moves through the root to airfoil transition region a shift in steady state location of the solidifying front is required to compensate for P/A ratio effects as shown in Figure 24. This analysis predicts that the solidification rate must decrease at the root to airfoil transition. In the case of plane front solidification of eutectics, theory predicts that in a lamellar system such as $\gamma' + \delta$ ($Ni_3Al - Ni_3Cb$) the solidification rate is related to the interlamellar spacing by $\lambda^2 R = c$ where λ = interlamellar spacing, R = solidification rate, c = constant. Therefore as the solidification rate decreases the interlamellar spacing should increase.

Figure 25 provides several photomicrographs of transverse sections through a fully lamellar $\gamma' + \delta$ eutectic turbine blade root to airfoil transition. Spacing measurements at 0.1 inch (.3 cm), 0.3 inch (0.8 cm) and 1.0 inch (2.54 cm) confirmed the fact that the solidification rate decreases from the nominal 1.0 inch/hr (2.54 cm/hr) to .55 in/hr (1.4 cm/hr) and returns to 1.0 inch/hr (2.54 cm/hr) in the middle of the airfoil as predicted by computer modeling.

As discussed in section II, it has been shown analytically that the liquid metal cooling process is basically heat input limited in that further increases in temperature gradient require the process to be operated at higher hot zone temperatures. Figure 26 shows this relationship for several tin bath temperature conditions.

This relationship has been experimentally quantified by direct measurement of temperature gradient on 0.5 inch (1.3 cm) diameter bars using the data reduction technique described previously. These results are shown in Figure 27. Figure 26 also predicts that for a fixed hot zone temperature the temperature gradient of the process should increase as the tin bath temperature decreases. This correlation has been validated experimentally in that it was found that at a fixed hot zone temperature of 2822°F (1550°C) the temperature gradient was improved 17 percent by decreasing the tin bath temperature from 536°F (280°C) to 464°F (240°C) in agreement with the trend predicted by heat transfer analysis.

Another interesting heat transfer result which has been confirmed by experimentation is that the temperature gradient present at the solidfying interface is a direct function of the P/A ratio of the casting being solidified. Figure 28 shows for selected hot zone temperatures how temperature gradient increases as the P/A ratio of the casting increases for fixed solidification rate and tin temperature conditions. This analysis predicts that for a fixed set of processing conditions the highest temperature gradients are present under high P/A conditions. Therefore, it is easier to achieve plane front solidification in an airfoil section of a blade as contrasted to the root. These results have been experimentally verified on eutectic turbine blades. Notice that the gradient predictions and results are consistent with the previous conclusion that we are dealing with a heat input limited process.

Computer simulation of directional solidification with the LMC process included an attempt to match the thermal profiles observed experimentally, see Figure 29. The calculated and experimental curves match in terms of thermal gradient at the eutectic temperature and roughly in terms of shape

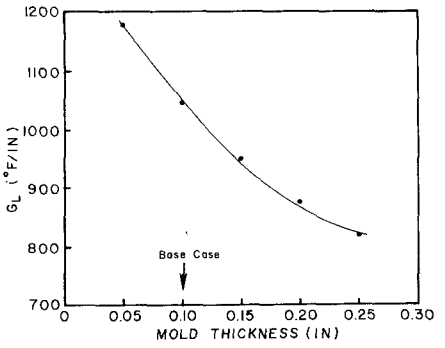

Figure 20. Analytical results for thermal gradient vs. mold thickness in the LMC process. Computed points have been fitted with a smooth curve.

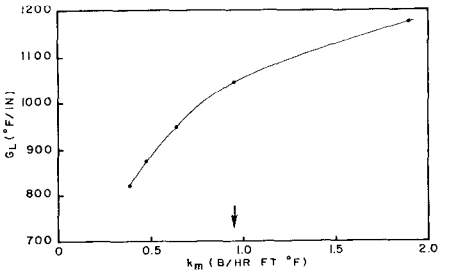

Figure 21. Analytical results for available thermal gradient in the liquid ahead of the eutectic interface as a function of the thermal conductivity of the mold. The base case of recrystallized aluminum oxide has been indicated.

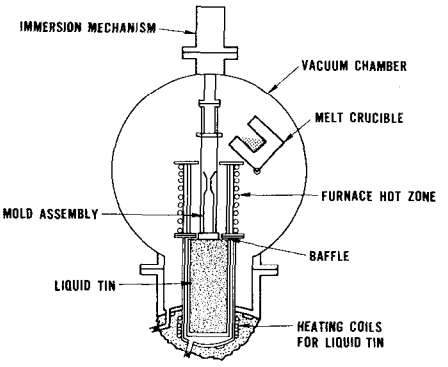

Figure 22. Scale-up version of the LMC directional solidification process with induction heated hot zone.

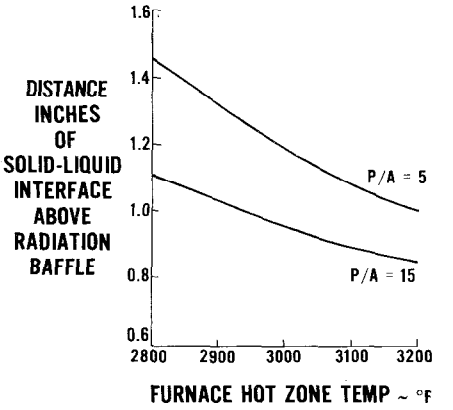

Figure 23. Analytical results from one dimensional heat flow model for interface position as a function of hot zone temperature with parameter P/A ratio.

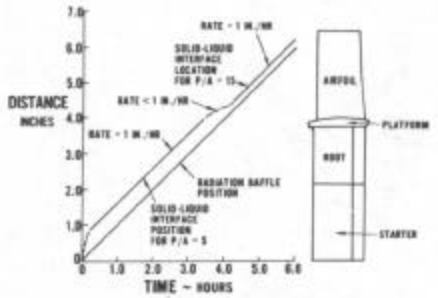

Figure 24. Effect of blade geometry on solidification. The difference in steady state positions for the two different P/A ratios leads to a growth rate transient at the change in section size. The problem has been simplified by regarding the platform simply as an extension of the root cross section.

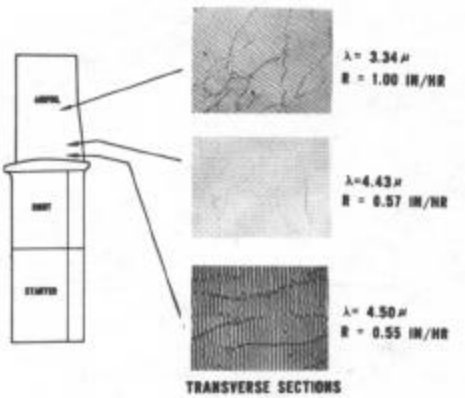

Figure 25. Microstructural confirmation of deceleration in growth velocity at the lower end of the airfoil section. The growth velocity has been computed from the observed interlamellar spacing.

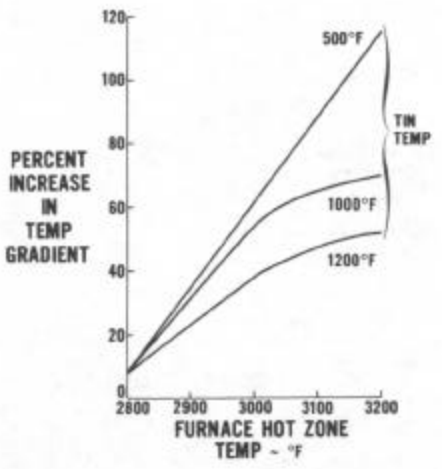

Figure 26. Analytical results for percent increase in thermal gradient from baseline conditions as a function of hot zone temperature with parameter tin bath temperature.

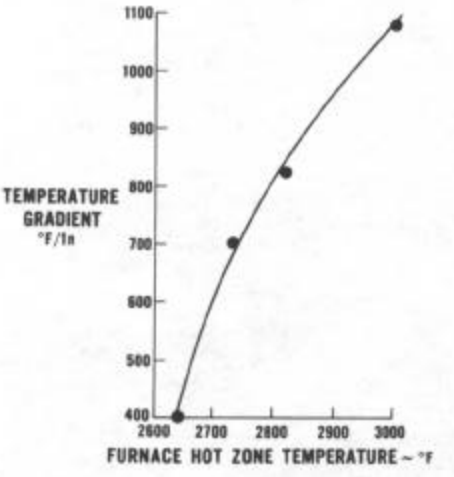

Figure 27. Experimental results from laboratory LMC unit for thermal gradient at the eutectic isotherm as a function of hot zone temperature.

in the baffle zone and in the hot zone. However, there are noticeable discrepancies in terms of interface position (about 0.4 in or 1.0 cm) and in terms of temperatures in the coolant zone. This disagreement indicates that the real system differs slightly from the idealized one. In the hot zone the computed interface position is below that observed (and the computed temperatures are too high). This is due to the fact that the actual hot zone is not uniform in temperature, but is actually cooler near the top of the baffles. This is an experimental condition which can be improved by profiling the hot zone. From a computational point of view, the non-uniform hot zone temperature must be taken into account, and this was successfully done with the finite difference method. The other difference can be explained in that the actual thermal contact between solidified alloy and mold is not as good as in the idealized case due to oxidation, mold fragmentation and alloy shrinkage. Therefore there is actually less cooling at the lower temperatures than would otherwise be expected. This can be taken into account computationally by adjusting the heat transfer coefficient to the bath.

The computer calculations continued to indicate that inadequate heat was being concentrated just above the baffles in the LMC process. The hot zone was therefore profiled by varying the turn density of the induction heating coil as indicated in Figure 30. In this case the high turn density region contains three times the number of turns per inch as the upper section of the heater. The application of this technique has allowed us to raise the thermal gradient from 600°F/in (133°C/cm) to 900°F/in (200°C/cm) within a relatively short period of time. There is an added benefit of lower hot zone temperatures in the low turn density region, namely a minimization of any mold-melt reaction. These measured thermal gradients have been thoroughly substantiated with microstructural measurements such as cellular to planar transitions for well documented high temperature eutectic alloy systems.

IV. Computerized Process Control

Another application of computers to the field of directional solidification is in the area of computerized process control. Computer control of directional solidification with either the HRS or LMC processes is an ideal application since both techniques approach steady state heat transfer conditions and are therefore readily programable. An example of a computer control system for the HRS process is depicted in Figure 31. In this case, thermal parameters which are programed into the system include melt temperature, hot zone control temperature and withdrawal rate. With these parameters the solidification variables such as temperature gradient, solidification rate, local solidification time, mushy zone width and cooling rate can be maintained at the desired values with a high degree of accuracy and reproducibility. The computer system also permits a full feedback capability which enables the process to be self regulating in the event that one of the parameters starts to deviate from the desired conditions. Other auxiliary control functions such as vacuum level, vacuum interlocks, electrical switching, introduction of inert gas and process water coolant monitoring can be efficiently programmed as well. This approach to process control is a natural blend of the detailed understanding of the directional solidification process and the thermal analysis methods discussed previously.

V. Summary

The high speed digital computer has contributed significantly to the improved understanding and control of directional solidification processing over the past seven years. The computer is used for thermal analysis (data reduction) in order to define growth rate, thermal gradient, interface position, mushy-zone height and local solidification time. These quantities have been correlated with changes in external variables to lead to process improvements. The improvement in thermal gradient, a key solidification variable, has been truly remarkable in progressing from power-down to high rate solidification to liquid metal cooling.

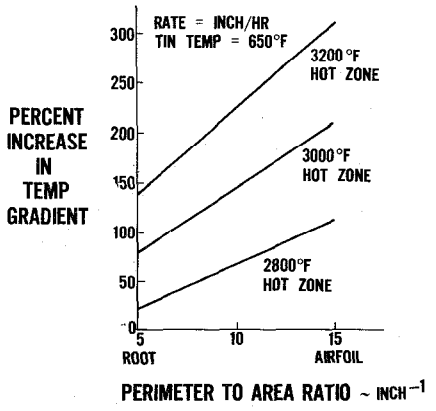

Figure 28. Analytical results for percent increase in thermal gradient as a function of perimeter to area ratio with hot zone temperature as a parameter.

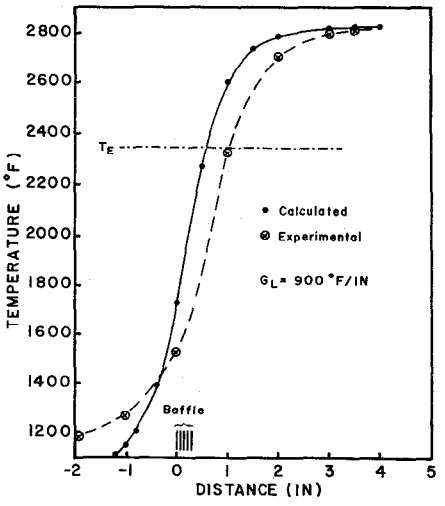

Figure 29. Calculated vs. experimental thermal profiles for LMC process. Computed results are from one dimensional model.

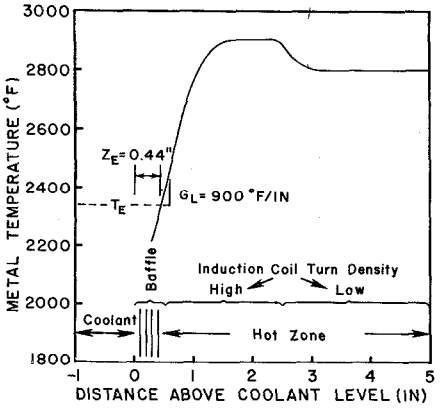

Figure 30. Experimental thermal profile showing the effects of variable turn density induction. The high to low turn density ratio was 3:1 in this case.

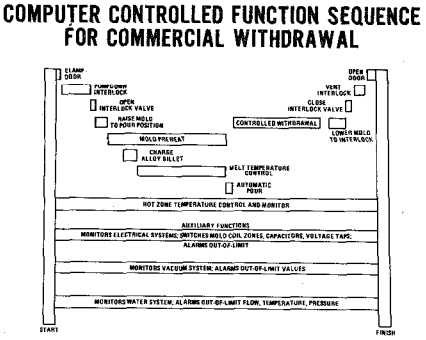

Figure 31. Diagram showing functions which could be computer controlled in the withdrawal version of directional solidification.

Another application for computers has been modeling, particularly for the LMC process. Finite element was successfully used for power-down and HRS with easy break-up and reasonable execution times. Finite difference was applied to the LMC process and was found to be informative, but cumbersome. Based on the finite difference information, a one dimensional steady state heat flow model was set up and a closed form analytical solution was obtained. This model has proved sufficiently accurate to be used as a predictive tool and is frequently used due to the large number of parametic variations which can be made with very little execution time. One does have to be careful in attempting to apply this model to extreme conditions where uniaxial heat flow may no longer occur at the solidification interface(s). Experimental checks of interface shape are helpful in this regard.

Comparisons of computed versus experimental results show excellent agreement in terms of thermal gradient and interface shape and reasonable agreement in terms of interface position for the LMC process. The predicted variations of thermal gradient with hot zone temperature, bath temperature, baffle thickness, mold thermal resistance, immersion rate and surface to volume ratio have all been verified experimentally. Detailed eutectic microstructures in complex shapes such as turbine blades agree very well with the predictions of the one dimensional model in that higher thermal gradients are obtained in airfoils than root sections and a growth rate (and interlamellar spacing) transient is observed at a geometry transition.

Finally, it would appear that computer control of the directional solidification process is just around the corner. This step should lead to the ultimate in process reproducibility.

Acknowledgement

The authors would like to sincerely thank B. H. Kear, R. A. Sprague and C. P. Sullivan for technical guidance. We would like to thank A. W. Forrest, L. S. Langston and J. G. Tschinkel for computational assistance. We are also indebted to L. F. Schulmeister, P. M. Curran and W. F. Gustafson for technical support. The authors are pleased to acknowledge the support of the Naval Air Systems Command in the area of directionally solidified eutectic turbine blades with Contracts N00019-73-C-0252 and N00019-74-C-0194.

References

1. F. L. VerSnyder in "High Temperature Materials", Ed. R. F. Hehemann and Mervin Ault, Wiley, New York, 1959.

2. B. H. Kear and B. J. Piearcey: Trans. TMS-AIME, 1967, Vol. 239, p. 1209.

3. F. L. VerSnyder and M. E. Shank: Mat. Sci. Eng., 1970, Vol. 6, p. 213.

4. A. F. Giamei and B. H. Kear: Met. Trans., 1970, Vol. 1, p. 2185

5. S. M. Copley, A. F. Giamei, S. M. Johnson and M. F. Hornbecker: Met. Trans., 1970, Vol. 1, p. 2193.

6. M. C. Flemings, R. V. Barone, S. Z. Urarnand and H. F. Taylor: Trans. Am. Foundrymen's Soc., 1961, Vol. 69, p. 422.

7. J. S. Erickson, W. A. Owczarski and P. M. Curran: Met. Prog., 1971, Vol. 99, p. 58.

8. F. D. Lemkey and E. R. Thompson in "Proceedings of the Conf. on In Situ Composites", NMAB 308-II, Nat. Acad. of Sci. and Eng'g., Washington, D. C., 1973.

9. E. R. Thompson, F. D. George and E. H. Kraft: NASC Final Report, Contract N00019-70-C-0052, July 1970.

10. A. F. Giamei and F. L. VerSnyder in "Grain Boundaries in Engineering Materials", Ed. J. L. Walter, J. H. Westbrook and D. A. Woodford, Claitor's Publ. Div., Baton Rouge, 1975.

11. A. F. Giamei, E. H. Kraft and F. D. Lemkey in "New Trends in Materials Processing", ASM Pre-Congress Seminar, Oct. 1974, in press.

12. T. Z. Kattamis, J. Coughlin and M. C. Flemings: Trans. TMS-AIME, 1967, Vol. 239, p. 1504.

13. K. H. Huebner: "The Finite Element Method for Engineers", Wiley, New York, 1976.

14. J. S. Erickson, C. P. Sullivan and F. L. VerSnyder in "High-Temperature Materials in Gas Turbines", Proc. Brown Boveri Sympos., Elsevier Sci. Publ. Co., Amsterdam, 1974.

15. M. N. Ozisik: "Boundary Value Problems of Heat Conduction", Int'l. Textbook Co., Scranton, 1968.

16. G. Liebman, ASME Paper No. 55-A-61, Nov. 1955.

17. P. M. Curran, L. F. Schulmeister, J. S. Erickson and A. F. Giamei: "Process Evaluation of Directionally Solidified Ni_3Cb Reinforced Eutectics in Turbine Blade Form", Final Report, Contract N00019-74-C-0194, March 1975.

18. P. M. Curran, L. F. Schulmeister, J. S. Erickson and A. F. Giamei: "An Investigation of Directional Solidification of Ni_3Cb Reinforced Eutectics in Complex Shapes", Ed. M. Jackson, J. Walter, R. Hertzberg and F. Lemkey, Proc. CISC-II, Xerox Publ. Co., Boston, in press.